

Biosorption of chromium (VI) from aqueous solutions and ANN modelling

Soma Nag¹ · Abhijit Mondal¹ · Nirjhar Bar² · Sudip Kumar Das²

Received: 9 February 2017 / Accepted: 19 May 2017 / Published online: 16 June 2017
© Springer-Verlag Berlin Heidelberg 2017

Abstract The use of sustainable, green and biodegradable natural wastes for Cr(VI) detoxification from the contaminated wastewater is considered as a challenging issue. The present research is aimed to assess the effectiveness of seven different natural biomaterials, such as jackfruit leaf, mango leaf, onion peel, garlic peel, bamboo leaf, acid treated rubber leaf and coconut shell powder, for Cr(VI) eradication from aqueous solution by biosorption process. Characterizations were conducted using SEM, BET and FTIR spectroscopy. The effects of operating parameters, viz., pH, initial Cr(VI) ion concentration, adsorbent dosages, contact time and temperature on metal removal efficiency, were studied. The biosorption mechanism was described by the pseudo-second-order model and Langmuir isotherm model. The biosorption process was exothermic, spontaneous and chemical (except garlic peel) in nature. The sequence of adsorption capacity was mango leaf > jackfruit leaf > acid treated rubber leaf > onion peel > bamboo leaf > garlic peel > coconut shell with maximum Langmuir adsorption capacity of 35.7 mg g⁻¹ for mango leaf. The treated effluent can be reused. Desorption study suggested effective reuse of the adsorbents up to three cycles, and safe disposal

method of the used adsorbents suggested biodegradability and sustainability of the process by reapplication of the spent adsorbent and ultimately leading towards zero wastages. The performances of the adsorbents were verified with wastewater from electroplating industry. The scale-up study reported for industrial applications. ANN modelling using multilayer perception with gradient descent (GD) and Levenberg-Marquart (LM) algorithm had been successfully used for prediction of Cr(VI) removal efficiency. The study explores the undiscovered potential of the natural waste materials for sustainable existence of small and medium sector industries, especially in the third world countries by protecting the environment by eco-innovation.

Keywords Detoxification · Adsorption · Chromium (VI) · Isotherm · ANN · Gradient descent · Levenberg-Marquart algorithm

Introduction

With the growth of industrial activity, the accumulation of heavy metals has been increased to a great extent. Process industries use various heavy metals and their traces remain present in wastewater. Water pollution due to disposal of industrial effluents is a global concern. The heavy metals are toxic, non-biodegradable and a threat to human health. So, detoxification of waste water at source is needed to protect the natural environment and to improve the quality of life of the people. Chromium is very toxic and used by many process industries. In aqueous systems, two oxidation states, viz., Cr(III) and Cr(VI), exist and have different chemical and biological properties. Cr(III) is relatively insoluble, whereas Cr(VI) is highly mobile in aqueous medium and very toxic to flora and fauna. Cr(VI) exposure causes diarrhoea, stomach

Responsible editor: Guilherme L. Dotto

Electronic supplementary material The online version of this article (doi:10.1007/s11356-017-9325-6) contains supplementary material, which is available to authorized users.

✉ Sudip Kumar Das
drsudipkdas@vsnl.net

¹ National Institute of Technology Agartala, Agartala, India

² Department of Chemical Engineering, University of Calcutta, Calcutta, India

and intestinal bleedings, cramps and liver and kidney damage and it is mutagenic (US Department of Health and Human Services 1991; Cieslak-Golonka 1995; Dakiky et al. 2002; Bhattacharya et al. 2008). The Cr(VI) present in industrial wastewater is found to be in the range of 0.5 to 270 mg L⁻¹ (Patterson 1985) and IS 10500 allows a discharge limit of 2 mg L⁻¹ in inland surface water (Indian Standard 1991).

Conventional removal methods used for Cr(VI) detoxification from wastewater are reduction and chemical precipitation (Özer et al. 1997), coagulation, solvent extraction (Mauri et al. 2001), ion exchange (Rengaraj et al. 2003), membrane separation (Padilla and Tavani 1999), electrolytic method (Namasivayam and Yamuna 1995), nanofiltration (Ahmed et al. 2006), etc. Each of these methods has advantages as well as disadvantages. Due to huge amount of sludge generation, precipitation method creates serious disposal problems (Dakiky et al. 2002). The ion exchange process is not suitable due to high cost of resin, while electrodeposition method requires high energy cost. Membrane scaling, fouling and blocking are the major problems in the membrane-based processes for wastewater treatment. Hence, it is seen that some are costly or not so effective at lower concentration of solute. Adsorption is found to be a very widely accepted method for wastewater treatment. The adsorbents should have strong affinity for metals to be removed with reasonably high adsorption capacity. So, researchers are trying to identify low-cost adsorbents with high metal binding affinity to replace the activated carbon or other costly adsorbents (Singha and Das 2011) in an eco-friendly manner which will not lead to any secondary pollution. The agricultural wastes, such as peanut husk, rice husk, rice straw and wheat bran, and different kinds of leaves, barks, fruit peels and seeds are tried by many researchers as low-cost adsorbent for removal of various heavy metals (Cimino et al. 2000; Dakiky et al. 2002; Dupont and Guillon 2003; Bhattacharya et al. 2008; Malkoc et al. 2006; Hasan et al. 2008; Murphy et al. 2008; Netzahuatl-Munoz et al. 2010; Singha and Das 2011; Netzahuatl-Munoz et al. 2012a, 2012b; Singh et al. 2014; Lopez-Nuñez et al. 2014; Şen et al. 2015; Netzahuatl-Munoz et al. 2015). In third world countries, a large number of very small- to medium-sized industries generate Cr(VI)-containing wastewater where the common or individual effluent treatment facility is not available. Hence, these industries need a low-cost process for their wastewater treatment and the use of natural biowaste materials turns out to be the best choice. This research programme has been undertaken to demonstrate the applicability of seven natural agricultural wastes as low-cost biosorbents for the removal of Cr(VI) from wastewater.

In recent years, the studies using artificial neural network (ANN) has become very popular for solving and modelling of different engineering problems due to capacity of handling complex and non-linear processes (Bar and Das 2011, 2013; Mitra et al. 2014; Singha et al. 2015; Bar and Das 2016). The

ANN is defined as “a data processing system consisting a large number of simple, highly interconnected processing elements (artificial neurones) in an architecture similar to the structure of the cerebral cortex of the brain” (Tsoukalas and Uhrig 1997). ANN models can learn from examples, incorporate large number of variables and give quick response related to new information. ANN are basically algorithms that perform non-linear statistical modelling and offer a number of advantages like less formal statistical training requirement, detection of complex non-linear relationship and all possible interactions between the variables and availability of number of training algorithms (Bar et al. 2010a). The major disadvantages are the “black box” and empirical nature, large computational time requirement, possibility of overfitting, etc. Bar et al. (2010a) and Bar and Das (2016) clearly demonstrated that ANN methodology has a superior modelling technique in comparison to the statistical modelling techniques where non-linear relation exists between the dependent and independent variables.

In this paper, seven naturally available agricultural wastes, e.g. jackfruit leaf, mango leaf, onion peel, garlic peel, bamboo leaf, sulphuric acid-treated rubber leaf and coconut shell, have been used as bio-adsorbents for estimation of their Cr(VI) removal efficiency from aqueous solution. ANN modelling using two training algorithms namely Gradient Descent and Levenberg-Marquardt has been implemented successfully.

Materials and methods

Collection and preparation of biosorbents

Tripura, India has a rich variety of horticulture/plantation crops. Orange, jackfruit, mango, pineapple, coconut, cashew nut, tea and rubber are produced in plenty (<http://www.agri.tripura.gov.in/tripurahtm>). Around 60% of the geographical area of Tripura, India is under forest coverage and 15% of the forest coverage has bamboo production. Every year, around 200,000 tonnes of bamboos of 19 varieties are produced in Tripura (<http://www.tfdpc.com/about2htm>). Due to the abundant availability of these, the leaves of jackfruit, mango, bamboo and rubber plant and coconut shell, onion peel and garlic peel were chosen as biosorbents for Cr(VI) removal. Leaves were collected from gardens near NIT Agartala, Tripura, India and the onion and garlic peels were collected from local markets. They were washed with distilled water to remove dirt and mud and sun-dried. Only the rubber leaf was pretreated with 0.1 N sulphuric acid for 4 h to remove colour and then washed with double distilled water. The dry leaves were ground and kept in an oven at 60 °C for 6 h. Finally, the powders were sieved to obtain particle size of -44 + 52 mesh (250–350 µm) and kept in airtight containers.

Preparation of standard Cr(VI) solution

Chromium (VI) stock solution (1000 mg L^{-1}) was prepared by dissolving 2.828 g of A.R. grade $\text{K}_2\text{Cr}_2\text{O}_7$ in de-ionized water. The standard and test solutions were prepared diluting this solution with de-ionized water. The synthetic aqueous solutions were used for study purpose.

Analysis of Cr(VI) ions

The absorbance of the standard Cr(VI) solutions was measured in a UV spectrophotometer at 540 nm, using 1,5-diphenylcarbazide as the colouring and complexing agent, and the calibration curve was prepared. The absorbance of the test solutions was measured (APHA 1998) with the help of calibration curve.

Reagents and equipment

All the chemicals used were from E. Merck India Limited, Mumbai, India. A digital pH meter (EUTECH make) was used to measure the pH of the solutions. The batch experiments were performed in an incubator shaker, and the absorbance of the Cr(VI) containing solution was read in a UV spectrophotometer at 540 nm (Lambda-25 UV-VIS, Perkin Elmer, USA).

Methodology

Specific gravity bottle, electric oven and muffle furnace were used to measure density, moisture and ash content of the biowaste materials, respectively. BET apparatus (Quantachrome Instruments, Micrometrics Instruments Corporation, USA) was used to find out the surface area for all the biosorbents by multilayer N_2 adsorption technique, and the surface morphology was studied by scanning electron microscope (SEM) (JSM-6390, JEOL, Japan). The point of zero charge on the biosorbent surfaces was measured by solid addition method (Singha and Das 2011; Zou and Zhao 2012) using 50-ml 0.1 mol L^{-1} KNO_3 solution and adjusting the initial pH (pH_i) between 2 and 11 by adding 0.1 N HCl or NaOH as per requirement. Of adsorbent powder, 0.2 g was added in each flask and stirred occasionally, and after 24 h, final pH was measured. The point of zero charge (pH_{pzc}) was obtained by plotting ΔpH vs pH_i at $\Delta\text{pH} = 0$.

Batch experiments

Batch study was conducted by taking 100-ml Cr(VI) solutions of known strength in 250-ml conical flasks and pH of the solutions were adjusted with 0.1 N H_2SO_4 or 0.1 N NaOH. The required quantities of biosorbents were added. The flasks were placed in the shaker and agitated at a constant speed of

110–120 strokes/min at $30 \pm 2 \text{ }^\circ\text{C}$. The flasks were taken out at a regular interval of time, and the Cr(VI) concentrations were measured, till equilibrium was reached. The experiments were repeated to investigate the effects of different operating parameters on the metal ion adsorption. The amount of Cr(VI) adsorbed on the biosorbent and percentage removal was calculated by the following equations:

$$q_t = \frac{(C_0 - C_t)V}{m_s} \quad (1)$$

$$\%_{\text{removal}} \text{ of Cr(VI) ions} = \frac{(C_0 - C_t)}{C_0} \times 100 \quad (2)$$

All the investigations were carried out in triplicate to ensure reproducibility ($\pm 0.5\%$) and relative deviation was $\pm 2.5\%$.

Results and discussion

Characterization

The physical properties of the biosorbents were measured in laboratory and reported in Table 1.

The SEM of the adsorbents (Fig. 1) indicates the irregular and porous structure on the adsorbent surfaces which took part in the metal adsorption.

The specific surface area, BET, of the adsorbents was determined by nitrogen adsorption/desorption isotherms, measured at 77 K. BET-specific surface area was evaluated encompassing external surface area and the pore area and was expressed in square meter per gram and reported in Table 1.

FTIR studies were conducted for all the fresh and Cr(VI) ion loaded biosorbents (Fig. S1 shows the FTIR plot for fresh and Cr(VI) loaded jackfruit leaf). Tables 2 and 3 represent the shift in the wave number of dominant peaks associated with the fresh and Cr(VI) loaded biosorbents from the FTIR plots. These shifts in the wave number show the presence of metal binding process at the surface of the biosorbents (Singha et al. 2011).

Effect of the operating parameters

To find out the effects of pH on Cr(VI) removal percentage, the studies were performed by varying the initial pH of the aqueous solution from 1 to 7 for each adsorbent, at initial Cr(VI) concentration of 20 mg L^{-1} and at $30 \pm 2 \text{ }^\circ\text{C}$ temperature. Adsorbents were added at a concentration of 5.0 g L^{-1} in each flask. Figure 2 shows that the Cr(VI) removal efficiency varies widely with pH of the solution and the maximum removal was observed at pH 2 for all biosorbents. Thereafter, the removal efficiency decreased sharply. The aqueous phase pH governs the metal removal efficiency due to the surface

Table 1 Characteristic of adsorbents

Name of adsorbent	Bulk density g cm^{-3}	BET surface area $\text{m}^2 \text{g}^{-1}$	p_{zpc}	Moisture content (dry basis) %	Ash content (dry basis) %
Jackfruit leaf	0.299	1.66	6.24	4.88	16.58
Mango leaf	0.367	2.38	6.82	5.86	12.94
Onion peel	0.191	5.95	4.02	6.47	4.99
Garlic peel	0.191	3.21	6.20	3.18	22.71
Bamboo leaf	0.214	11.52	6.20	4.10	12.00
Treated rubber leaf	0.279	6.96	7.22	5.44	4.50
Coconut shell	0.683	1.49	6.62	4.56	3.28

properties of the biosorbents and the performance of the active functional groups. This may be due to the fact that at low pH, the dominant form of Cr(VI) was HCrO_4^- . The increase in pH shifted the concentration of HCrO_4^- to $\text{Cr}_2\text{O}_7^{2-}$ and CrO_4^{2-} . At low pH, a large number of H^+ ions were present, which neutralized the OH^- ions on the adsorbent surface and facilitated diffusion and adsorption of Cr(VI) ions on the adsorbent surface (Nag et al. 2016; Bhattacharya et al. 2008). In general, adsorption of cation is favoured at $\text{pH} < \text{pH}_{pzc}$ (Bhattacharya et al. 2008; Singha and Das 2011). Hence for rest of the studies, the aqueous solution pH is maintained at pH 2 to get the maximum biosorption.

The effect of adsorbent type and its concentration was studied by varying the adsorbent dosing from 0.5 to 10 g L^{-1} in 100 ml of 20 mg L^{-1} concentrated solutions of Cr(VI). Figure 3 shows that the percent removal increases with the

increase in adsorbent concentration and reaches its maximum value at a concentration of 10 g L^{-1} . However, for the four adsorbents, viz., jackfruit leaf, mango leaf, acid-treated rubber leaf and onion peel, there were no significant increases in the removal efficiency after dosages of 2 g L^{-1} . For the other adsorbents, viz., bamboo leaf, garlic peel and coconut shell, optimum adsorbent concentration was 5 g L^{-1} . It may be explained that with an increase in biosorbent dosages, more surface area were available for biosorption so that the removal efficiency increased.

The effect of contact time on batch adsorption at pH 2 and biosorbent dosages of 5 g L^{-1} is presented in Fig. 4. The percentage removal increased with time and the initial removal rate was very fast. Thereafter, the reaction rate became slow and reached equilibrium slowly. The 90% of the reaction for the jackfruit leaf, mango leaf, acid-treated rubber leaf and

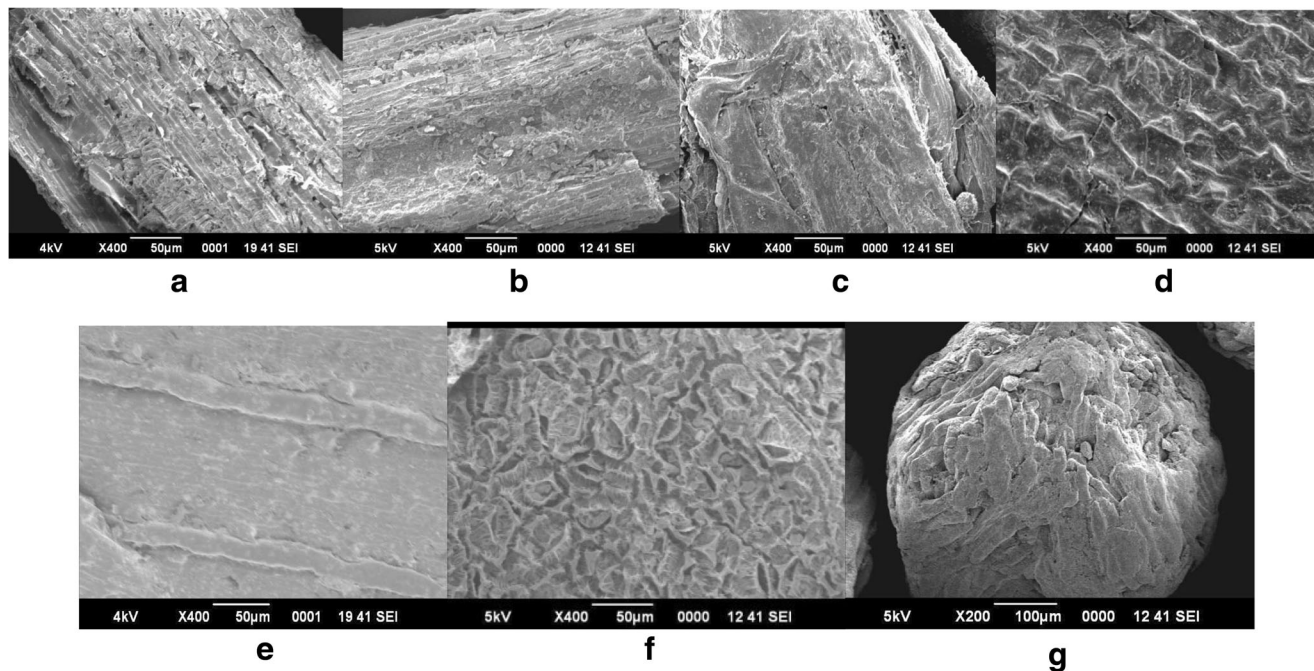


Fig. 1 Scanning electron micrograph (SEM) of the adsorbents. **a** Jackfruit leaf. **b** Mango leaf. **c** Onion peel. **d** Garlic peel. **e** Bamboo leaf. **f** Treated rubber leaf. **g** Coconut shell

Table 2 FTIR analysis of fresh and Cr(VI) loaded adsorbents

Functional group	Jackfruit leaf		Mango leaf		Onion peel		Garlic peel	
	Fresh	Cr(VI) loaded	Fresh	Cr(VI) loaded	Fresh	Cr(VI) loaded	Fresh	Cr(VI) loaded
Surface O-H stretching	3277.18	3290.35	3246.32	3310.95	3254.09	3278.07	3269.37	3319.24
Aliphatic C-H stretching	2915.55	2915.57	2916.35	2915.53	–	–	2914.55	2916.39
Aldehyde C-H stretching	2848.32	2847.27	2848.18	2847.95	2848.87	2849.62	–	–
Aliphatic C=O stretching	1730.15	1729.75	–	–	–	–	–	–
Amine N-H stretching	1619.87	1622.13	–	–	1607.25	1735.38	1608.09	1646.55
α-CH ₂ bending	–	–	–	–	–	–	1416.99	1416.87
Carboxylic acid and derivatives O-C stretching	–	–	1228.66	1224.62	1221.90	1216.57	1315.49	1230.47
								1316.29
								1258.33
Sulphonic acid S=O stretching	1031.79	1031.87	1031.22	1017.09	–	–	–	–
Amine C-N stretching	–	–	–	–	1005.62	1008.41	1007.09	1009.73

onion peel were completed within half an hour. For the rest three adsorbents, i.e. bamboo leaf, garlic peel and the coconut shell, the reaction rate was moderate and it took nearly 4 h to attain equilibrium.

The Cr(VI) removal percentage decrease with an increase in initial metal ion concentration may be due to saturation of the active sites as more Cr(VI) ions were present in higher concentrations (Fig. 5). At higher concentration, more Cr(VI) ions remained un-adsorbed. However, the equilibrium adsorption capacity, q_e (mg g⁻¹), increased with an increase in initial Cr(VI) ion concentration could be due to an increase in electrostatic interactions.

Reaction kinetics

Reaction orders were determined using different kinetic models, and the model parameters were calculated and

reported in Table 4 along with the correlation coefficients. The models are as under:

Pseudo-first-order Lagergren model

The model (Lagergren 1898) assumed that the adsorption was controlled by diffusion and was expressed by,

$$\log(q_e - q_t) = \log q_e - \frac{k_1}{2.303} t \tag{3}$$

The plot of $\log(q_e - q)$ vs t (Fig. S2) was used to find out the model parameters and reported in Table 4.

Pseudo-second-order model

This model (Ho and Mckay 2000) assumed that chemisorptions took place on the adsorbent surface and was expressed by,

Table 3 FTIR analysis of fresh and Cr(VI) loaded adsorbents

Functional group	Bamboo leaf		Treated rubber leaf		Coconut shell	
	Fresh	Cr(VI) loaded	Fresh	Cr(VI) loaded	Fresh	Cr(VI) loaded
Surface O-H stretching	3306.17	3291.19	3279.65	3296.14	–	–
Aliphatic C-H stretching	2915.90	2925.17	2916.13	2915.47	–	–
Aldehyde C-H stretching	2848.52	2839.47	2848.29	2824.12	–	–
Phosphite ester group	–	–	–	–	2354.15	2359.32
Aliphatic C=O stretching	–	–	–	–	1718.53	1715.21
Amine N-H stretching	1634.87	1624.48	1634.50	1622.24	–	–
Aromatic C-NO ₂ stretching	–	–	–	–	1507.98	1507.31
Alkane group stretching	–	–	–	–	1471.76	1455.30
Carboxylic acid and derivatives O-C stretching	–	–	1229.23	1247.70	–	–
Sulphonic acid S=O stretching	1032.32	1032.60	1030.82	1029.79	1030.29	1032.29

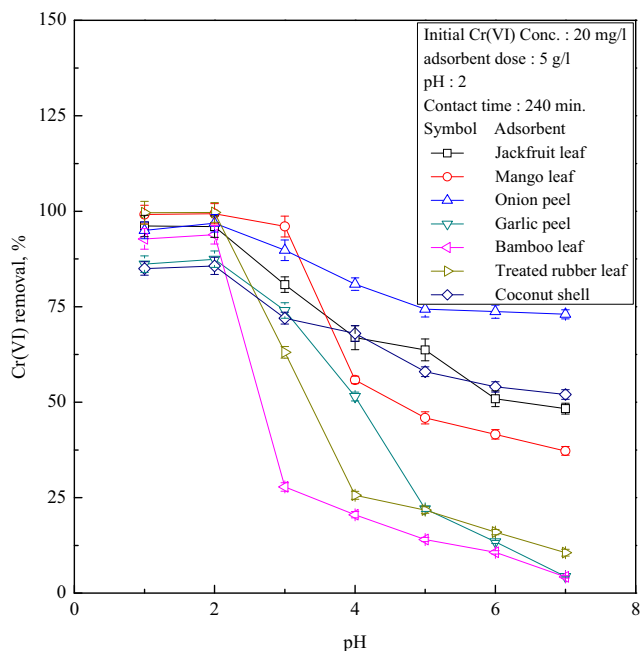


Fig. 2 Effect of pH on removal of Cr(VI) for different adsorbents

$$\frac{t}{q_t} = \frac{1}{k_2 q_e^2} + \frac{t}{q_e} \quad (4)$$

The parameters were determined from the plot of $\frac{t}{q_t}$ vs t (Fig. S3), and the values of the rate constants are presented in Table 4. The high correlation coefficient indicated that the pseudo-second-order model represented the experimental data better than first-order model for all the biosorbents.

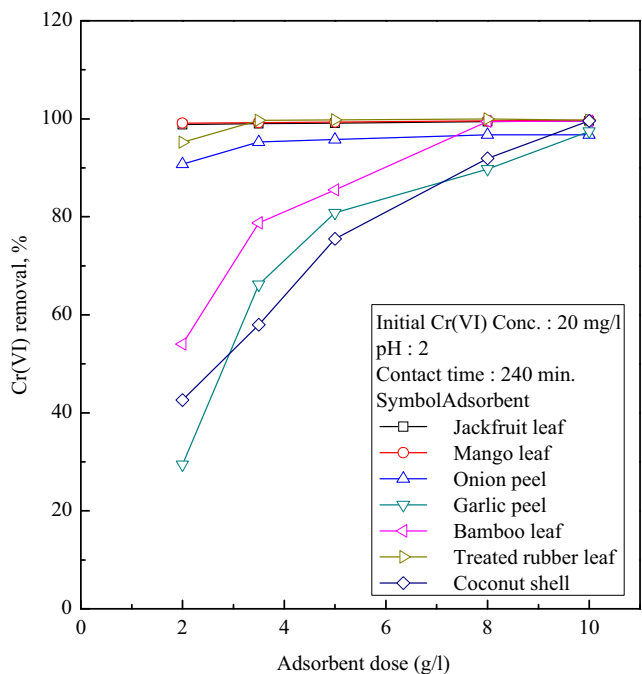


Fig. 3 Effect of adsorbent dosage on removal of Cr(VI) for different adsorbents

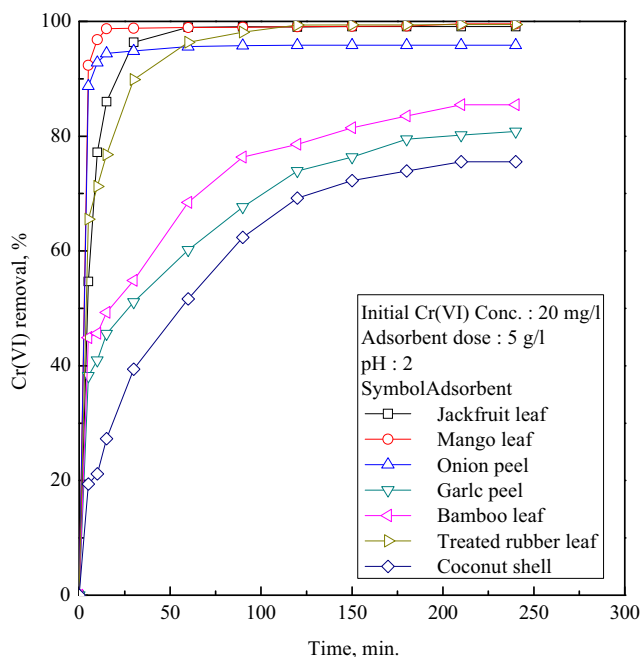


Fig. 4 Effect of contact time on removal of Cr(VI) for different adsorbents

Intraparticle diffusion model

The biosorption may be controlled by one or more steps. Sometimes, it is seen that for initial period of reaction, the intraparticle diffusion is the rate-limiting step. This possibility was explored by using the model developed by Weber and Moris (1963) as,

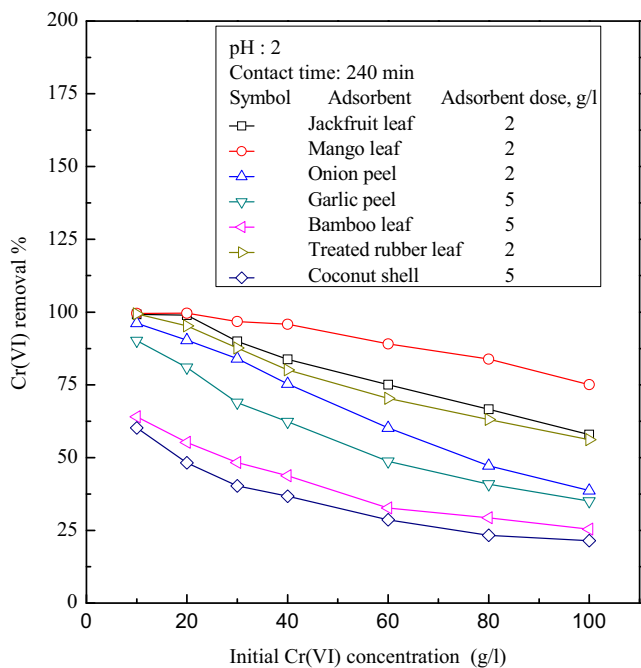


Fig. 5 Effect initial Cr(VI) concentration on removal

Table 4 Different kinetic model parameters

Model constants	Jackfruit leaf	Mango leaf	Onion peel	Garlic peel	Bamboo leaf	Treated rubber leaf	Coconut shell
Pseudo 1st-order Lagergren model: $\log(q_e - q) = \log q_e - \frac{K_1 t}{2.303}$							
K_1 (min ⁻¹)	0.0643	0.0115	0.0553	0.0196	0.0170	0.0448	0.0211
R^2	0.8286	0.4340	0.9615	0.9570	0.9634	0.9714	0.9842
Pseudo 2nd-order model: $\frac{t}{q} = \frac{t}{q} + \frac{t}{q}$							
K_2 (mg g ⁻¹ min ⁻¹)	0.1045	0.6669	0.8034	0.0175	0.0198	0.0629	0.0094
R^2	0.999	0.999	0.999	0.995	0.997	0.999	0.994
Intraparticle diffusion model: $q = K_{id} t^{0.5}$							
K_{id} (mg g ⁻¹ min ^{-0.5})	0.8295	0.1583	0.1506	0.1402	0.3272	0.1733	0.2672
R^2	0.9429	0.9526	0.9408	0.9354	0.9941	0.9932	0.9800
Elovich model: $q_t = \left(\frac{1}{b_1}\right) \ln(a_1 b_1) + \left(\frac{1}{b_1}\right) \ln t$							
a_1	5.99	2.13	3.20	3.91	1.86	23.99	1.30
b_1	3.04	0.50	12.72	3.53	2.44	3.66	2.03
R^2	0.8446	0.9821	0.7474	0.8874	0.9472	0.9821	0.9001
Richenberg model: $F = \left(1 - \frac{6}{\pi}\right) e^{-Bt} Bt = -0.4977 \ln(1 - F)$							
R^2	0.9844	0.9939	0.9970	0.9777	0.9878	0.9896	0.9877

$$q_t = k_{id} t^{0.5} + C_{id} \tag{5}$$

C_{id} represents external convective mass transfer from the bulk liquid to the surface of the solid and related to boundary layer thickness (the greater the C_{id} , the greater is the boundary layer effect). These parameters were obtained by fitting q_t against square root of time. If a good fit is obtained and if the plot passes through origin ($C_{id} = 0$), then according to Weber and Moris (1963), the intraparticle diffusion is the rate-limiting step. The plot of q_t vs $t^{0.5}$ of experimental data showed multi-linear segments, which indicated that the biosorption process was controlled by more than one phenomenon. The high correlation coefficient for the initial phase of reactions indicated the dominance of the intraparticle diffusion. The slope of the initial linear portion was used to find out the rate parameter, k_{id} , and is reported at Table 4.

Elovich model

Elovich model was involved previously for chemical adsorption of gases on solid surface without desorption of the products, so the rate of adsorption decreased with time due to surface coverage. The model is applicable in case of chemisorptions (Ho and McKay 2002) and is given by Wu et al. (2009),

$$q_t = \left(\frac{1}{b_1}\right) \ln(a_1 b_1) + \left(\frac{1}{b_1}\right) \ln t \tag{6}$$

The model parameters were determined from the plot of $\ln t$ vs q_t and are reported at Table 4 along with the correlation coefficients. The model appeared to be significant for the

biosorbents, viz., jackfruit leaf, bamboo leaf, treated rubber leaf and coconut shell. For others, this model was not that significant.

Biosorption mass transfer

Prediction of rate of adsorption is the most important factor in adsorption system design. The adsorption mechanism depends upon the surface characteristics of the adsorbents and the mass transfer rate. The functional groups present on the adsorbent surfaces control the adsorption process. The sorption of adsorbate by an adsorbent consists of film diffusion process, i.e. transport of adsorbate from the solution to the film surrounded the solid adsorbent, external diffusion, i.e. diffusion of the adsorbate from the film to the solid adsorbent, intraparticle transport, i.e. diffusion from the surface of the adsorbent to its internal sites, and finally pore diffusion, i.e. adsorption of the adsorbate to its interior pores.

Prediction of adsorption rate-limiting step

The prediction of rate-limiting step in adsorption process is an important criterion. Generally, the inner or outer diffusion controls the adsorption rate. To describe the diffusion process of Cr(VI) ions on the micropores of the biosorbents, Fick’s equation was attempted (Singha and Das 2011),

$$\frac{q_t}{q_\infty} = \frac{6}{R_a} \sqrt{\frac{D_e t}{\pi}} \tag{7}$$

q_∞ is replaced by q_e and the plot of q_t/q_e vs $t^{0.5}$ of experimental data showed multi-linear segments (Fig. 6). The first

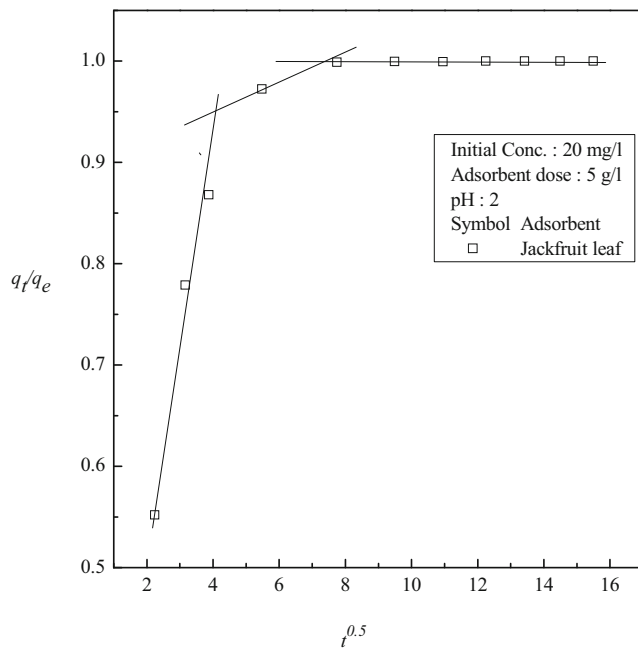


Fig. 6 Plot of q_t/q_e vs $t^{0.5}$

steeper portion represented the diffusion mass transfer and the second linear portion indicated the intraparticle diffusion and the last linear portion were related to adsorption-desorption equilibrium (Singha and Das 2011). The time required for each part was calculated from the plot, and it was observed that the first linear portion took 1.95 min and the second linear portion took 3.4 min for jackfruit leaf. The ratio of the time taken by film diffusion to intraparticle diffusion was 3:5. So, it was concluded that intraparticle diffusion was predominant over the film diffusion and intraparticle diffusion was the rate controlling step for adsorption of Cr(VI) on jackfruit leaf. Similarly, the segmental time taken was calculated for other adsorbents. The ratio of the time taken by film diffusion to intraparticle diffusion was 1:2, 2:5, 2:1, 1:3, 3:4 and 11:7 for treated rubber leaf, mango leaf, bamboo leaf, onion peel, garlic peel and coconut shell, respectively. So, the intraparticle diffusion was rate-controlling step for jackfruit leaf, mango leaf, onion peel, garlic peel and treated rubber leaf, whereas for bamboo leaf and coconut shell, film diffusion was predominant and was the rate-limiting step.

Determination of diffusivity coefficient

The diffusion kinetic model equation, represented by Eq. (8), was applied for biosorption of Cr(VI) from aqueous solution, assuming spherical shape of the biosorbents (Singha and Das 2013),

$$\ln \left[\frac{1}{1-F^2(t)} \right] = \frac{\pi^2}{R_a^2} D_e t \quad (8)$$

From the plot of $\ln \left[\frac{1}{1-F^2(t)} \right]$ vs t , the diffusivity coefficient (D_e) was determined and shown in Table 5.

Richenberg model

This model assumed that for fast reactions, sorption occurred due to mass transfer by film diffusion and in the pores of the adsorbent. The rate of sorption was given by the Eq. (9) (Singha and Das 2013),

$$F = \left(1 - \frac{6}{\pi^2} \right) e^{-Bt} \quad (9)$$

The equation was rewritten as,

$$Bt = -0.4977 \ln(1-F) \quad (10)$$

The plot of Bt vs time for all the seven adsorbents was linear in nature for the initial part of the adsorption and the correlation coefficients were depicted in Table 4. The linear correlation shown by the plots indicated the predominance of film and intraparticle diffusion in controlling the sorption rate.

Mass transfer analysis

Mass transfer analysis was carried out by using the equation proposed by Ho et al. (2000),

$$\begin{aligned} & \ln \left(\frac{C_t}{C_0} - \frac{1}{1 + MK_{bq}} \right) \\ &= \ln \left(\frac{1}{1 + MK_{bq}} \right) - \ln \left(\frac{1 + MK_{bq}^{bq}}{MK_{bq}} \right) \beta St \quad (11) \end{aligned}$$

The plot of $\ln \left(\frac{C_t}{C_0} - \frac{1}{1 + MK_{bq}} \right)$ vs t yielded a straight line and from the slope, $\ln \left(\frac{1 + MK_{bq}^{bq}}{MK_{bq}} \right) \beta S$, the value of mass transfer coefficient (β) was calculated. Values of mass transfer coefficient were estimated for all the biosorbents and are presented in Table 5. The values indicated that the mass transfer from the liquid phase to the solid phase was quite fast.

The biosorption isotherms

The isotherm models were used to predict the equilibrium relationship between the Cr(VI) ions in the aqueous solution and its adsorption on the solid adsorbent at constant temperature. The adsorption capacity predicted by these isotherm models shows the feasibility of a given application at optimum operating conditions and also provides an important design parameter for scale-up modelling (Dinçer et al. 2007; Giwa et al. 2013; Singha and Das 2013). The equilibrium studies were conducted at initial Cr(VI) ion concentration range of

Table 5 Values of diffusion and mass transfer coefficient

Parameters	Jackfruit leaf	Mango leaf	Onion peel	Garlic peel	Bamboo leaf	Treated rubber leaf	Coconut shell
Diffusion coefficient, D_e ($\times 10^{10}$ m ² s ⁻¹)	1.4080	0.5386	1.2369	0.02784	0.3537	1.2711	0.3560
Mass transfer coefficient, β ($\times 10^6$ cm s ⁻¹)	0.92	0.18	1.74	0.08	0.11	1.09	1.53

10–100 mg L⁻¹ under isothermal conditions. The optimum biosorbent dosages as obtained earlier were used for this study, i.e. 2 g L⁻¹ for mango leaf, jackfruit leaf, onion peel and treated rubber leaf and 5 g L⁻¹ for rest of the biosorbents. Experimental data were correlated with Langmuir, Freundlich, Temkin and Dubinin-Radushkevich models.

Langmuir isotherm model

Langmuir (1918) model assumed monolayer adsorption with a finite number of homogeneous adsorption sites. It refers to homogeneous adsorption and each molecule possess constant enthalpies and sorption activation energy (Kundu and Gupta 2006). Linearity of the plot indicated the applicability of the isotherm. The equation is commonly written as follows,

$$\frac{C_e}{q_e} = \frac{C_e}{q_{max}} + \frac{1}{q_{max}b} \tag{12}$$

From the slope and intercept of the linear plot of $\frac{C_e}{q_e}$ vs C_e , the values of q_{max} and b were determined for all the adsorbents (Fig. S4) and presented in Table 6. The essential characteristics and feasibility of Langmuir isotherm were expressed by a dimensionless constant, called separation factor (Singha and Das 2011), R_L , which is defined as,

$$R_L = \frac{1}{1 + bC_0} \tag{13}$$

The R_L value lying between 0 and 1 indicates strong affinity for adsorption. All the values of R_L were less than 1, which indicated favourable biosorption.

Freundlich isotherm model (Freundlich 1906)

Freundlich model is applied to multilayer adsorption with non-uniform adsorption heat distribution. Freundlich equation is given by,

Table 6 Different isotherm constants

Model constants	Jackfruit leaf	Mango leaf	Onion peel	Garlic peel	Bamboo leaf	Treated rubber leaf	Coconut shell
Langmuir isotherm model: $\frac{C_e}{q_e} = \frac{C_e}{q_e} + \frac{C_e}{q_e}$							
q_{max} , mg g ⁻¹	32.29	35.70	19.88	9.22	10.76	29.79	8.73
b , L mg ⁻¹	0.3036	0.4529	0.2913	0.1084	0.1402	0.3537	0.0995
R^2	0.9717	0.9845	0.9768	0.9336	0.9228	0.9839	0.8896
Separation factor: $R_L = \frac{1}{1+bC_0}$							
R_L value for Cr(VI) concentration of 10 mg L ⁻¹	0.2478	0.1555	0.2556	0.4799	0.4164	0.2204	0.5014
R_L value for Cr(VI) concentration of 100 mg L ⁻¹	0.0319	0.0181	0.0332	0.0845	0.0666	0.0275	0.0914
Freundlich isotherm model: $\log q_e = \log K_f + \frac{1}{n} \log C_e$							
K_f (mg g ⁻¹)/(mg L ⁻¹) ^{1/n}	11.3084	15.1775	6.8884	2.4978	3.4538	10.5696	2.5389
n	3.7799	4.0586	3.7790	3.7456	4.4695	3.7389	4.2061
R^2	0.9186	0.9811	0.9348	0.9273	0.8895	0.9834	0.8722
Temkin isotherm model: $q_e = b_T \ln K_T + b_T \ln C_e$							
b_T , J mol ⁻¹	3.85	5.48	5.45	1.21	1.68	3.98	1.40
K_T , L mg ⁻¹	82.27	32.65	0.91	3.159	1.80	7.32	1.21
R^2	0.9774	0.9841	0.9267	0.9315	0.9125	0.9516	0.8632
Dubinin-Radushkevich isotherm model: $\ln C_{abs} = \ln X_m - \lambda \epsilon^2$; $\epsilon = RT \ln \left(1 + \frac{1}{C_e} \right)$; $E = \frac{1}{\sqrt{2\lambda}}$							
E , kJ mol ⁻¹	9.10	8.26	8.31	6.04	11.22	9.63	9.66
X_m , mg g ⁻¹	0.60	0.74	0.28	0.11	0.10	0.36	0.08
R^2	0.9168	0.9587	0.7007	0.9662	0.6640	0.8676	0.6397

Table 7 Thermodynamic parameters

Parameters	Temperature K	Jackfruit leaf	Mango leaf	Onion peel	Garlic peel	Bamboo leaf	Treated rubber leaf	Coconut Shell
$-\Delta G^0$ kJ mol ⁻¹	303	12.71	12.06	5.07	3.86	4.37	7.14	4.60
	313	14.90	13.12	5.99	4.19	8.38	10.64	5.24
	323	16.25	13.71	8.04	5.03	8.98	13.73	6.67
ΔH^0 kJ mol ⁻¹		40.12	83.03	39.71	13.72	65.54	92.78	26.73
ΔS^0 J mol ⁻¹ K ⁻¹		174.98	83.07	147.24	57.75	232.51	330.00	103.00

$$\log q_e = \log K_f + \frac{1}{n} \log C_e \quad (14)$$

K_f and n were calculated for all the adsorbents from the Freundlich plot (Fig. S5) and reported in Table 6. The values of n lying between 1 and 10 indicated favourable biosorption, and for the tested biosorbents, the n value was 3.7389 for treated rubber leaf (minimum value) and 4.4695 (maximum value) for the bamboo leaf. The greater the value of n , the greater is the expected heterogeneity.

Temkin isotherm model

The model considers that the heat of adsorption decreases with an increase in surface coverage (Temkin and Pyzhev 1940) and is represented by,

$$q_e = b_T \ln K_T + b_T \ln C_e \quad (15)$$

From the plot of q_e vs $\ln C_e$, Temkin model constants were evaluated and represented in Table 6. The heat of adsorption (b_T) is directly related to the coverage of Cr(VI) on the biosorbents due to biosorbent-biosorbate interaction.

From the comparison of the models, the higher correlation coefficient, R^2 , indicates that Langmuir and Temkin model fitted well compared to Freundlich model for most of the adsorbents. However, for treated rubber leaf and onion peel, equivalent results were obtained in all the models.

Dubinin-Radushkevich isotherm model (Dubinin et al. 1947)

This model is applied to express the adsorption mechanism, i.e. whether physical or chemical (Gunay et al. 2007; Dubinin 1960). The linear form of model is described by,

$$\ln q_e = \ln q_m - \lambda \varepsilon^2 \quad (16)$$

Where the Polanyi potential (Polanyi 1932), ε , is given by,

$$\varepsilon = RT \ln \left(1 + \frac{1}{C_e} \right) \quad (17)$$

From the plot of $\ln q_e$ vs ε^2 , the values of λ and q_m were calculated from slope and intercept, respectively. The mean sorption energy, E , was evaluated from,

$$E = \frac{1}{\sqrt{2\lambda}} \quad (18)$$

The numerical values of sorption energy, E , determine whether the process was physical or chemical. If the value of E is less than 8 kJ/mol, the process is physical biosorption, and if the value lies between 8 and 16, it indicates chemisorptions. The estimated value of E (Table 6) indicated the biosorption process was chemical for all the adsorbents except garlic peel (Singha and Das 2011).

Table 8 Desorption of Cr(VI) from loaded adsorbents

Strength of NaOH M	Adsorbent						
	Jackfruit leaf	Mango leaf	Onion peel	Garlic peel	Bamboo leaf	Treated rubber leaf	Coconut shell
0.05	10.76	9.54	12.65	6.98	6.87	8.67	16.34
0.10	12.74	14.87	13.98	8.45	8.53	13.70	17.92
0.20	15.43	18.34	15.64	11.94	10.54	15.65	19.32
0.25	17.32	20.02	17.35	14.65	11.43	16.78	22.71
0.40	20.32	25.32	18.03	16.32	14.76	22.78	23.87
0.50	21.63	26.56	19.54	17.54	16.72	24.54	24.64
0.75	23.79	30.65	19.76	18.43	18.60	29.61	25.78

Table 9 Regeneration of adsorbent

Adsorbent	Cr(VI) removal percentage, %		
	Initial Cr(VI) concentration = 10 mg L ⁻¹ , adsorbent dose = 5 g L ⁻¹ , pH = 2		
	Fresh	After 1st regeneration	After 2nd regeneration
Jackfruit leaf	99.8	87.6	43.2
Mango leaf	99.1	86.5	59.0
Onion peel	87.2	69.2	32.1
Garlic peel	80.9	61.5	40.3
Bamboo leaf	92.5	80.1	56.7
Treated Rubber leaf	97.0	61.9	32.3
Coconut shell	83.4	69.1	49.2

Thermodynamic studies

Studies were conducted at three temperatures 30, 40 and 50 °C for initial Cr(VI) concentration range of 10–100 mg L⁻¹. The thermodynamic equilibrium constant, K_C^0 , was obtained by calculating apparent equilibrium constant, K'_C , at different temperature and initial Cr(VI) concentration for each system and extrapolating to zero different initial concentrations and then extrapolated to zero (Bhattacharya et al. 2008). The thermodynamic parameters, such as, Gibbs free energy (ΔG°), enthalpy (ΔH°) and entropy (ΔS°) were determined by using the following equations,

$$K'_c = \frac{C_{ad}}{C_e} \tag{19}$$

$$\Delta G^0 = -RT \ln K_C^0 \tag{20}$$

The Gibbs free energy (ΔG°) was calculated from Eq. (20), and its negative value suggested the spontaneous nature of the biosorption process and its further decrease with temperature indicated that the spontaneity increased with increasing temperature. The enthalpy (ΔH°) and entropy were calculated from the slope and the intercept of the plots of $\ln K_C^0$ vs $1/T$ for the respective adsorbents.

$$\ln K_C^0 = -\frac{\Delta H^0}{RT} + \frac{\Delta S^0}{R} \tag{21}$$

Positive values of ΔH° and ΔS° change suggested that the biosorption process was endothermic and random in nature. Moreover, the value of enthalpy change suggested that the biosorption of Cr(VI) on garlic peel was physical in nature and the rest of it was chemisorptions. If the heat of biosorption is between 2.1 and 20.9 kJ/mol, then the process is physical, and if the value lies in between 20.9 and 418.4 kJ/mol, the process is chemical (Kondapalli and Mohanty 2011). All the values are reported in Table 7.

Desorption studies

The used adsorbents were regenerated by adding different concentration of NaOH solutions (0.05–0.75 M). It was found that desorption started at pH \geq 8. Table 8 shows that the higher concentration of NaOH was required to increase the Cr(VI) desorption efficiency. Similar results were obtained by other researchers (Singha and Das 2011). The alkali desorption clearly suggested that the adsorption was chemical in nature. The Cr(VI) ions remained on the biosorbent surface due to

Table 10 Analysis of electroplating wastewater using adsorbents

Parameters	Untreated effluent	Treated effluent						
		Jackfruit leaf	Mango leaf	Onion peel	Garlic peel	Bamboo leaf	Treated rubber leaf	Coconut shell
pH	5.95	2.18	2.43	2.24	2.14	2.41	2.22	2.30
Cr(VI), mg L ⁻¹	51.89	4.44	3.45	5.25	8.65	8.82	4.39	6.67
Cu(II), mg L ⁻¹	5.24	3.41	4.98	5.04	5.07	4.32	3.76	5.02
Ca(II), mg L ⁻¹	22.73	20.86	21.32	20.87	21.19	21.65	21.92	20.21
Na(I), mg L ⁻¹	154.32	129.76	132.65	138.56	130.54	140.25	138.67	134.61
K(I), mg L ⁻¹	1.93	1.32	1.21	1.06	1.01	1.58	1.03	0.94
Zn(II), mg L ⁻¹	0.94	0.69	0.65	0.73	0.75	0.64	0.53	0.62
TDS, mg L ⁻¹	854	795	813	807	818	780	802	794

Table 11 Comparison of adsorption capacities of natural/agricultural adsorbents

Serial no.	Adsorbents	Adsorption capacities for Cr(VI) mg g ⁻¹	Reference
1	Walnut shell	1.33	Orhan and Büyükgüngör (1993)
2	Neem sawdust	58.82	Orhan and Büyükgüngör (1993)
3	Sugar beet pulp	17.2	Sharma and Foster (1994)
4	Maize cob	13.8	Sharma and Foster (1994)
5	Saw dust	16.05	Bailey et al. (1999)
6	Hazelnut shell	17.7	Dönmez and Aksu (2002)
7	Wool	41.15	Dakiky et al. (2002)
8	Olive cake	33.44	Dakiky et al. (2002)
9	Saw dust	15.82	Dakiky et al. (2002)
10	Pine needles	21.5	Dakiky et al. (2002)
11	Almond	10.61	Dakiky et al. (2002)
12	Cactus	7.08	Dakiky et al. (2002)
13	Beech sawdust	16.1	Acar and Malkoc (2004)
14	Peanut husk	7.00	Dubey and Gopal (2007)
15	Neem leaf	7.43	Venkateswarlu et al. (2007)
16	Saw dust	20.70	Bhattacharya et al. (2008)
17	Neem bark	19.60	Bhattacharya et al. (2008)
18	Almond shell	3.40	Pehlivan and Altun (2008)
19	Hazelnut shell	8.28	Pehlivan and Altun (2008)
20	Wallnut shell	8.01	Pehlivan and Altun (2008)
21	<i>Catla catla</i> scales	29.18	Kondapalli and Mohanty (2009)
22	Groundnut hull	30.21	Qaiser et al. (2009)
23	Wheat straw	21.34	Wang et al. (2010)
24	Rice straw	12.172	Singha and Das (2011)
25	Rice bran	12.341	Singha and Das (2011)
26	Rice husk	11.398	Singha and Das (2011)
27	Hyacinth roots	15.281	Singha and Das (2011)
28	Neem leaves	15.954	Singha and Das (2011)
29	Fish scale	5.69	Kondapalli and Mohanty (2011)
30	Custard apple peel powder	7.87	Krishna and Sree (2013)
31	<i>Pistia stratiotes</i> Biomass	7.24	Das et al. (2013)
32	<i>Ficus carica</i> bark	19.68	Gupta et al. (2013)
33	Bagasse	25.15	Gupta and Majumder (2014)
34	Rubber leaf	22.97	Nag et al. (2016)
35	Jackfruit leaves	32.29	Present study
36	Mango leaves	35.70	Present study
37	Onion peel	19.88	Present study
38	Garlic peel	9.22	Present study
39	Bamboo leaves	10.76	Present study
40	Treated rubber leaves	29.79	Present study
41	Coconut shell	8.73	Present study

strong bond formation with biosorbents. The regenerated biosorbents were recycled for reuse and ultimately they were incinerated. Table 9 shows the performance of the regenerated biosorbents. The alkali addition may provide additional activation in the un-adsorbed part of the biosorbents; hence,

biosorption was higher in the case of first regeneration and was reduced very fast subsequently, whereas efficiency of the Cr(VI) removal for acid-treated rubber leaf was low. Adsorption/desorption cycle of the biosorbents decreased as the number of cycle increased. Although regeneration is

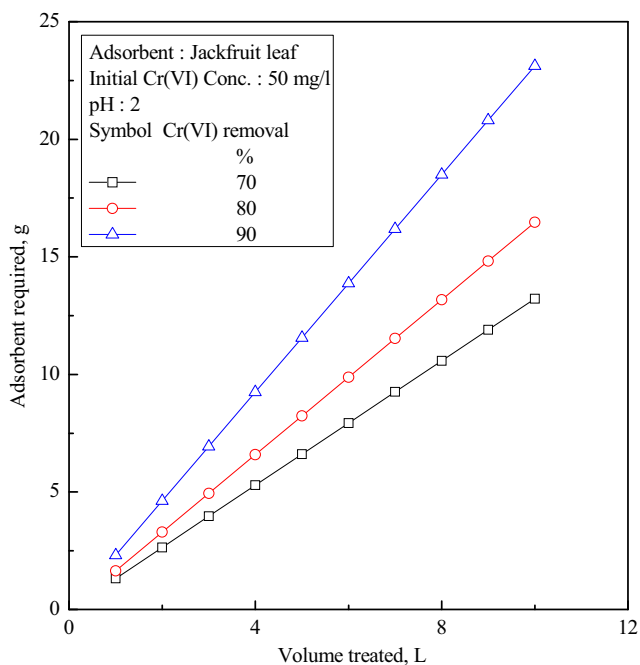


Fig. 7 Scale-up design for jackfruit leaf

feasible, however, the same is not recommended as the biosorbents are easily available in nature in abundant quantities without any cost and their maximum usages will clean-up the environment.

Application studies using electroplating wastewater

The wastewater was collected from a small scale electroplating unit from Dum Dum, Kolkata, West Bengal and was tested for the applicability of the biosorbents in batch condition. In terms of removal efficiency, the mango leaf showed the best performance (99.13%) and bamboo leaf had the minimum (83.00%) among all the biosorbents studied (Table 10).

Comparison of the adsorption capacities

The results obtained in this study were compared with the adsorption capacities of various other natural adsorbents reported in literature and are shown in Table 11. It may be noted that the adsorption capacity varied widely due to various

Table 13 Range of data

Measurement type		Range
Input parameters	Adsorbent dosage (g L ⁻¹)	0.5 to 10.0
	pH	1 to 7
	Initial concentration C ₀ (mg L ⁻¹)	5.00 to 100
	Time t (min)	5 to 270
Output parameter	Percentage removal (%)	4.32 to 100.00
Total number of data points		258

process parameters and the characteristics of individual adsorbents.

Single-stage batch biosorption system design

The mass balance equation for biosorption of Cr(VI) on the adsorbent surface from the aqueous solution at any point of time may be written as (Singha and Das 2013),

$$V(C_0 - C_t) = W(q_t - q_0) \tag{22}$$

If fresh biosorbents are used, q₀ = 0, so Eq. (18) reduces to,

$$V(C_0 - C_t) = Wq_t \tag{23}$$

When the system reaches equilibrium, the equation may be rewritten as,

$$V(C_0 - C_e) = Wq_e \tag{24}$$

Since the biosorption systems followed Langmuir adsorption isotherm relationship better for all the biosorbents discussed here, the model was used for designing of the batch biosorption system. The Langmuir equilibrium relationship is given by Eq. (12), and combining with Eq. (24), the following equation is obtained,

$$\frac{W}{V} = \frac{(C_0 - C_e)(bC_e + 1)}{bC_e q_{max}} \tag{25}$$

From the sets of known values of b and q_{max} for the individual biosorbents, the Eq. (24) was further simplified and a relationship for W/V was obtained in terms of C₀ and C_e. Fig. 7 shows the plot of mass of jackfruit leaf required

Table 12 Mass of adsorbents required for 80% removal of Cr(VI) from 20 mg L⁻¹ Cr(VI) solution

Volume of effluent, L	Jackfruit leaf	Mango leaf	Onion peel	Garlic peel	Bamboo leaf	Treated rubber leaf	Coconut shell
2	1.8070	1.3912	2.9911	11.4752	8.2770	1.8334	12.8754
4	3.6140	2.7824	5.9822	22.9504	16.5540	3.6668	25.7508
6	5.4210	4.1736	8.9733	34.4256	24.8310	5.5002	38.6262
8	7.2280	5.5648	11.9644	45.9008	33.1080	7.3336	51.5016
10	9.0350	6.9560	14.9560	57.3760	41.3850	9.1670	64.3770

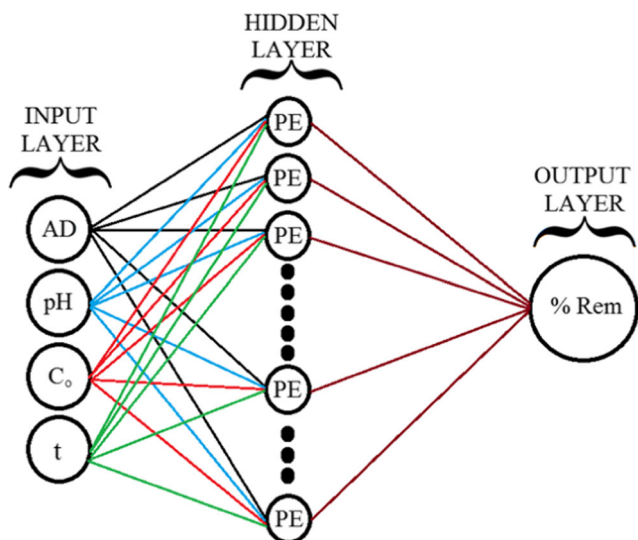


Fig. 8 Schematic diagram of ANN

for removal of Cr(VI) for aqueous solution containing 50 mg L⁻¹ Cr(VI) ion for 70, 80 and 90% removal of Cr(VI) at different volume of solutions (1–10 L). The amount of different biosorbents required for 80% removal of Cr(VI) ion from 20 mg L⁻¹ Cr(VI) aqueous solution is tabulated in Table 12.

Safe disposal of used biosorbents

The leaching possibility of the chromium ions from the used biosorbents restricts its dumping in the open environment. The Cr(VI) loaded biosorbents were incinerated at 700 °C to form ash and then 5 mg of the ash samples was mixed with 25 ml of de-ionized water to give a liquid–solid ratio of 5:1 (Sarode et al. 2010; Nag et al. 2016). After continuous gentle stirring for 24 h, the filtrate was analysed for Cr(VI) ions. It was observed that Cr(VI) did not leach from the ash sample. Hence, this ash may be used for road filling particularly in the nearby rural areas or to be placed in the agricultural field or may be used as fuel. Thus, the

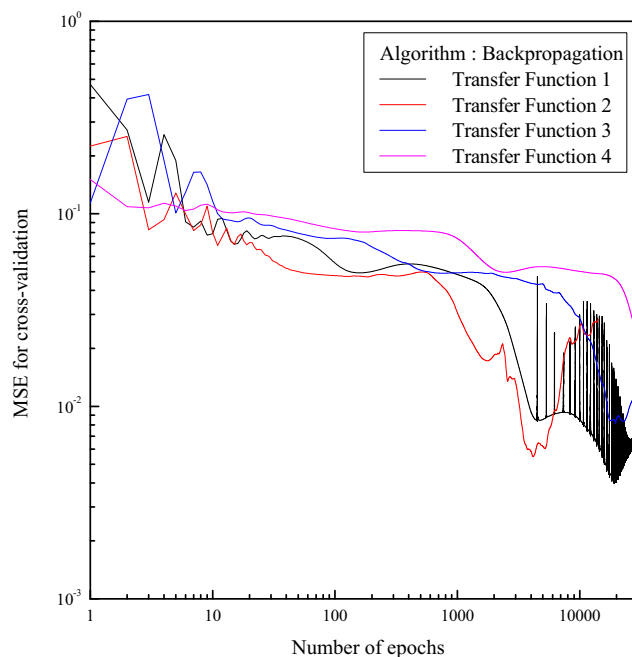


Fig. 9 Cross-validation curves for gradient descent algorithm

reapplication of the spent biosorbents will approach towards zero secondary pollution.

ANN modelling

Table 13 represents the input and output parameters used for ANN study along with the range of variables investigated. Considering the popularity and usefulness of the algorithms, the present study is done using gradient descent (GD) and Levenberg-Marquardt (LM) algorithm. The gradient descent and Levenberg-Marquardt algorithms are to find the local minimum of the function which may not be the global minimum. The gradient descent algorithm starts picking an arbitrary initial set of parameter values within the function’s range and take small steps towards the direction of greatest slope

Table 14 Optimum numbers of processing elements in the hidden layer for four different transfer functions

Transfer function in hidden layer	Equation	Algorithm	Optimum number of processing elements
Transfer function 1	$f_{1h}(x) = \tanh \beta x = \frac{e^{\beta x} - e^{-\beta x}}{e^{\beta x} + e^{-\beta x}}$	GD LM	14 14
Transfer function 2	$f_{2h}(x) = \beta x$ Where $\beta x = 1$ for $\beta x > 1$ $\beta x = -1$ for $\beta x < -1$	GD LM	23 18
Transfer function 3	$f_{3h}(x) = \beta x$ Where $\beta x = 0$ for $\beta x < 0$ $\beta x = 1$ for $\beta x > 1$	GD LM	24 18
Transfer function 4	$f_{4h}(x) = \frac{1}{1 + e^{-\beta x}}$	GD LM	8 13

GD Gradient Descent, LM Levenberg-Marquart

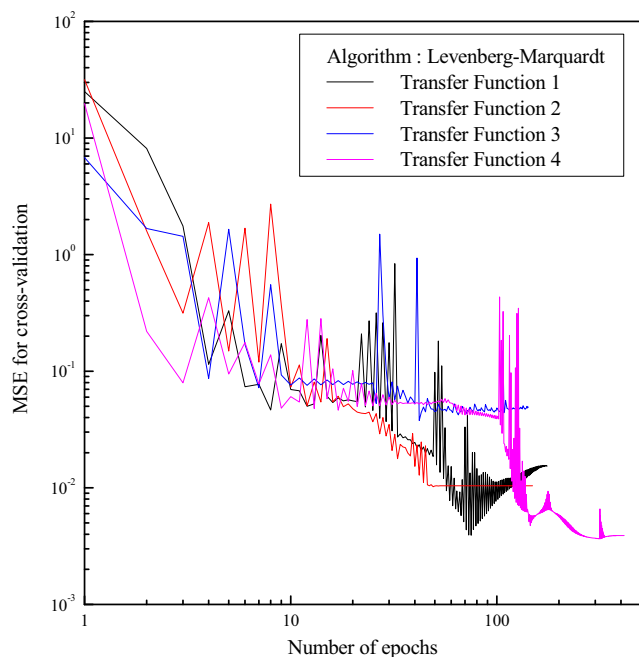


Fig. 10 Cross-validation curves for Levenberg-Marquardt algorithm

changes, which is the negative direction of the function gradient, and eventually, after many iterations, reaches to the minimum of the function. The Levenberg-Marquardt

algorithm is a pseudo-second-order method as it works only with the function evaluations and gradient information. It is combination of the gradient descent and the Gauss-Newton method. 70% (181), 20% (52) and 10% (25) data points were used for training, cross-validation and testing, respectively, for both the algorithms used. The training of the algorithm is necessary to define the procedure to be adopted to find the desired behaviour by the modification of the synaptic weights and to learn from the environment to improve their performance. Each algorithm has its own set of rules for training. The cross-validation is the performance of the ANN, and it is to be monitored up to the satisfactory optimum point then stop the training (Gordon 1994). It is a valuable technique to avoid overfitting in the ANN training process (Gordon 1994; Yang 2007).

ANN performance

Figure 8 shows the schematic diagram of the ANN. The input and output parameters are shown in this schematic diagram. From our previous experience (Mitra et al. 2014; Singha et al. 2014), it is concluded that normalization using Eq. (26) yields better prediction. The normalization was done using the following relation,

$$\text{Normalised value} = 10 + \left(\frac{\text{Input} - \text{minimum input value}}{\text{Maximum input value} - \text{minimum input value}} \times 10 \right) \tag{26}$$

The input variables were biosorbent dosages, pH, initial concentration and time, and the output variable was the percentage removal of Cr(VI). The stopping criterion of training and cross-validation was considered so that there was no threshold value required, but it depends on the improvement of the Mean Squared Error (MSE) value within 10,000 and 100 epochs, respectively, for GD and LM algorithm, respectively.

For the better performance, the statistical parameters of the network output, i.e. the values of MSE, Average Absolute Relative Error (AARE) and standard deviation, are expected to be small. The verification of the value of cross-correlation

coefficient between input and output (as much close to 1 as possible) was done.

Figure S6 shows how the change of minimum value of cross-validation MSE occurs with the number of nodes for the transfer functions used in the hidden layer for Levenberg-Marquardt algorithm. For the analysis with gradient descent algorithm, similar procedure was followed. The optimum number of processing element was estimated by taking into account the minimum value of MSE for cross-validation, and these numbers were represented in Table 14. From the cross-validation curve of the neural networks using

Table 15 Performance of the best neural network on the basis of minimum value of MSE reached during cross-validation

Transfer function in hidden layer	Algorithm	
	Gradient descent	Levenberg-Marquardt
Transfer function 1	0.003961	0.003918
Transfer function 2	0.005479	0.010234
Transfer function 3	0.008176	0.037760
Transfer function 4	0.020958	0.003663

Table 16 Performance of the different algorithms for prediction of percentage removal of Cr(VI) bed height by the optimized neural network

Transfer function in hidden layer	Measurement type	Algorithm	
		Gradient descent	Levenberg-Marquardt
Transfer function 1	AARE	0.051943	0.028726
	SD (σ)	0.053712	0.022620
	MSE	1.627158	0.378164
	CCC (R)	0.884903	0.962956
Transfer function 2	AARE	0.038186	0.063010
	SD (σ)	0.042351	0.052688
	MSE	0.978410	1.820671
	CCC (R)	0.922598	0.854681
Transfer function 3	AARE	0.047957	0.071104
	SD (σ)	0.035068	0.056749
	MSE	1.036677	2.037310
	CCC (R)	0.904787	0.764614
Transfer function 4	AARE	0.069871	0.042723
	SD (σ)	0.051550	0.054922
	MSE	2.095403	1.270299
	CCC (R)	0.820491	0.907863

gradient descent algorithm (Fig. 9) and Levenberg-Marquardt algorithms (Fig. 10), the gradual decrease of MSE was observed. It was also observed that the training was stopped abruptly because of the lack of improvement of the cross-validation MSE value.

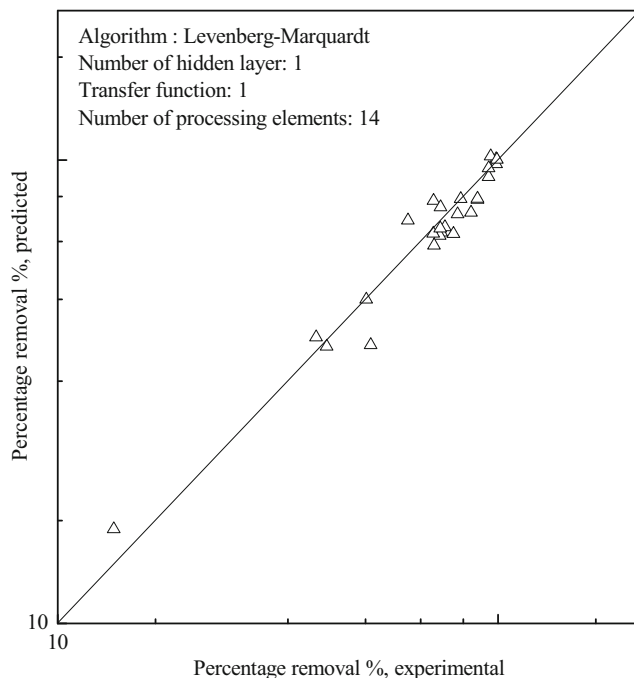
**Fig. 11** Comparison between the experimental to the predicted percentage removal

Table 15 represents the minimum value of cross-validation MSE reached during training with all the transfer functions. Similar type of procedure was reported earlier (Bar et al. 2010a, b; Bar and Das 2011, 2013; Mitra et al. 2014; Singha et al. 2014, 2015; Das et al. 2015).

From the observation related to the values of AARE, SD, MSE and cross-correlation coefficient (R) from Table 16, it was clear that the transfer function 1 with 14 optimum number of processing elements gives the most accurate prediction of the percentage removal when Levenberg-Marquardt algorithm is used. Figure 11 shows the comparison between the experimental to the predicted percentage removal. This result indicated that the performance of the network output is per excellence.

Conclusion

In this study, experiments were conducted using all locally available agricultural/natural waste materials, for Cr(VI) removal from aqueous solution at different process parameters, such as initial pH, biosorbent dose, initial Cr(VI) concentration, contact time, temperature, etc. in batch operation. The results may be summarized as follows:

1. The removal of Cr(VI) from aqueous solution strongly depends upon pH of the solution. The optimum pH was 2.
2. Metal removal efficiency was quite high for the biosorbents and the adsorption efficiency increased with an increase in adsorbent dosage. Almost 100% removal of Cr(VI) was possible at specified process parameters.

3. Different adsorption capacity was noted for different biosorbents and the highest adsorption capacity of 35.70 mg g⁻¹ was obtained for mango leaf.
4. The pseudo-second-order model fitted better than the first order model.
5. Langmuir adsorption isotherm was found to be more appropriate than Freundlich or Temkin model, indicating monolayer adsorption.
6. Langmuir q_{max} value indicated that the adsorption capability decreased in the following order: mango leaf > jackfruit leaf > treated rubber leaf > onion peel > bamboo leaf > garlic peel > coconut shell.
7. Calculated sorption energy from Dubinin-Radushkevich isotherm model indicated the chemical nature of the sorption process for all except garlic peel.
8. Thermodynamic parameters revealed the spontaneity, randomness and endothermic nature of the biosorption process.
9. Standard enthalpy change also suggested for chemisorption process except garlic peel.
10. The biosorbents were found suitable for treating industrial electroplating wastewater successfully.
11. The mango leaf had the maximum Cr(VI) removal efficiency (99.13%) and bamboo leaf had minimum removal efficiency (83.00%) among all the adsorbents studied for wastewater from electroplating industries.
12. Desorption studies using NaOH solution have been reported.
13. Scale-up study has also been reported.
14. The results obtained in this study are comparable with the adsorbents reported in the literature.
15. The practical utility of the biosorbents was proved on industrial wastewater.
16. Safe disposal study highlighted the eco-friendliness of the biosorbents
17. The major utility of this study is that the findings may be beneficial to the local small scale units by the way of treating their Cr(VI)-contaminated effluents.
18. Applicability of ANN modelling is successfully demonstrated.
19. ANN modelling showed that Levenberg-Marquardt algorithm with transfer function 1 having one hidden layer with 14 processing elements predicts the percentage removal of Cr(VI) with acceptable statistical accuracy in both the training and prediction abilities.
20. Finally, the study revealed the undiscovered potential of different local biowaste materials in an innovative way to combat the challenging environmental issues in a sustainable management.

ΔpH , Difference of pH; ΔG^0 , Gibbs free energy (kJ mol⁻¹); ΔH^0 , Enthalpy (kJ mol⁻¹); ΔS^0 , Entropy (J (mol K⁻¹)⁻¹);

AARE, Average Absolute Relative Error $AARE = \frac{1}{N} \sum_{i=1}^N \left| \frac{y_i}{\hat{y}_i} \right|$, dimensionless; a_1 , Elovich constant which gives an idea of the reaction rate constant, (mg g⁻¹ min⁻¹); b , Langmuir constant (L mg⁻¹); b_1 , Elovich constants and represents the rate of chemisorptions at zero coverage (g mg⁻¹); b_T , Temkin constant related to heat of sorption (J mol⁻¹); C_{id} , Constant in Eq. (5); C_{ad} , Cr(VI) concentration on adsorbent at time t (mg L⁻¹); $C_{ad,eq}$, Concentration of Cr(VI) on the adsorbent at equilibrium (mg L⁻¹); C_e , Cr(VI) concentration in solution at equilibrium (mg L⁻¹); C_o , Initial Cr(VI) concentration in solution (mg L⁻¹); C_t , Cr(VI) concentration in solution at any time, t (mg L⁻¹); D_e , Effective diffusion coefficient of absorbate in the absorbent phase (m² s⁻¹); E , Mean Sorption Energy (kJ mol⁻¹); E_a , Apparent activation energy (kJ mol⁻¹); F , Ratio of amount of Cr(VI) ion adsorbed per g of biosorbent at any time to that of equilibrium time; k_1 , Lagergren rate constant (min⁻¹); k_2 , Pseudo-second-order rate constant (g mg⁻¹ min⁻¹); k_{id} , Intraparticle rate constant (mg g⁻¹ min^{-0.5}); K_{bq} , The constant obtained by multiplying q_{max} and b ; K_c^0 , Thermodynamic equilibrium constant; K_c^l , Apparent equilibrium constant; K_F , Freundlich constant (mg/g)/(mg/l)^{1/n}; K_T , Temkin isotherm equilibrium binding constant (L g⁻¹); M , Mass of the adsorbent per unit volume (g L⁻¹); MSE, Mean Squared Error, $MSE = \frac{1}{N} \sum_{i=1}^N (x_i - y_i)^2$, dimensionless; m_s , Mass of adsorbent added in g; n , Freundlich constant, intensity of adsorption [(mg g⁻¹)/(mg L⁻¹)^{1/n}]; pH_{pzc} , Point of zero charge; q_e , q_α , Amount adsorbed (mg) per g of adsorbent at equilibrium (mg g⁻¹); q_m , Maximum adsorption capacity (mg g⁻¹); q_{max} , Maximum adsorption capacity (mg g⁻¹); q_t , Amount adsorbed (mg) per g of adsorbent at time t (mg g⁻¹); q , Metal uptake capacity (mg g⁻¹); R , Cross-correlation coefficient, $R = \frac{\sum_{i=1}^N (x_i - \bar{x})(y_i - \bar{y})}{\sqrt{\sum_{i=1}^N (x_i - \bar{x})^2 \sum_{i=1}^N (y_i - \bar{y})^2}}$, dimensionless; R^2 , Correlation coefficient; R , Ideal gas constant (J mol⁻¹ K⁻¹); R_L , Separation factor; R_a , Radius of adsorbent particle (m); S_s , External surface area of the adsorbent per unit volume (m⁻¹); t , Time (min); T , Temperature (K); V , Volume of the solution in millilitre; β , Mass transfer coefficient (cm s⁻¹); ϵ , Polanyi potential (kJ² mol⁻²); λ , Activity coefficient constant related to sorption energy (mol² kJ⁻²); $\sigma = \sqrt{\frac{1}{N-1} \sum_{i=1}^N \left[\frac{1}{|N-1|} - AARE \right]^2}$, dimensionless

References

- Acer FN, Malkoc E (2004) The removal of chromium (VI) from aqueous solution by fagus orientalis L. Bioresour Technol 94:13–15
- Ahmed MT, Taha S, Chaabane T, Akretche D, Maachi R, Dorange D (2006) Nanofiltration process applied to the tannery solutions. Desalination 200(1–3):419–420

- APHA, AWWA, WEF (1998) Standard methods for examination of water and wastewater, 20th edn. Washington D.C., New York
- Bailey SE, Olin TJ, Bricka RM, Adrian DD (1999) A review of potentially low-cost sorbents for heavy metals. *Water Res* 33:2469–2479
- Bar N, Das SK (2011) Comparative study of friction factor by prediction of frictional pressure drop per unit length using empirical correlation and ANN for gas-non-Newtonian liquid flow through 180° circular bend. *Int Review Chem Eng* 3(6):628–643
- Bar N, Das SK (2013) Frictional pressure drop for gas-non-Newtonian liquid flow through 90° and 135° circular bend: prediction using empirical correlation and ANN. *Int J Fluid Mech Res* 39(5):416–437
- Bar N, Das, S.K., 2016. Applicability of ANN in adsorptive removal of Cd(II) from aqueous solution. In: J. K Mandal, S. Mukhopadhyay, T. Pal (Eds), Handbook of research on natural computing for optimization, , Vol. II, pp 554–592, IGI Global book series Advances in Computational Intelligence and Robotics (ACIR) (ISSN: 2327-0411; eISSN: 2327-042X), IGI Global, USA.
- Bar N, Bandyopadhyay TK, Das SK, Biswas MN (2010a) Prediction of pressure drop using artificial neural network for non-Newtonian liquid flow through piping components. *J Pet Sci Eng* 71(3):187–194
- Bar N, Das SK, Biswas MN (2010b) Prediction of pressure drop using artificial neural network for gas non-Newtonian liquid flow through piping components. *Ind Eng Chem Res* 49(19):9423–9429
- Bhattacharya AK, Naiya TK, Mandal SN, Das SK (2008) Adsorption kinetics and equilibrium studies on removal of Cr(VI) from aqueous solutions using different low-cost adsorbents. *Chem Eng J* 137(3): 529–541
- Cieslak-Golonka M (1995) Toxic and mutagenic effects of chromium (VI) A review. *Polyhedron* 15(21):3667–3689
- Cimino G, Passerini A, Toscano G (2000) Removal of toxic cations and Cr(VI) from aqueous solution by hazelnut shell. *Water Res* 34(11): 2955–2962
- Dakiky M, Khamis M, Manassra A, Mereb M (2002) Selective adsorption of chromium (IV) in industrial waste water using low cost abundantly available adsorbents. *Adv Environ Res* 6(4):533–540
- Das B, Mondal NK, Roy P, Chattaraj S (2013) Equilibrium, kinetic and thermodynamic study on chromium (VI) removal from aqueous solution using *Pistia stratiotes* biomass. *Chem Sci Trans* 2:85–104
- Das B, Ganguly UP, Bar N, Das SK (2015) Holdup prediction in inverse fluidization using non-Newtonian pseudoplastic liquids: empirical correlation and ANN modeling. *Powder Technol* 273(C):83–90
- Dinçer AR, Güneş Y, Karakaya N, Güneş E (2007) Comparison of activated carbon and bottom ash for removal of reactive dye from aqueous solution. *Bioresour Technol* 98(4):834–939
- Dönmez D, Aksu Z (2002) Removal of chromium (VI) from saline wastewater by dunaliella species. *Process Biochem* 38(5):751–762
- Dubey SP, Gopal G (2007) Adsorption of chromium (VI) on low cost adsorbents derived from agricultural waste materials: a comparative study. *J Hazard Mater* 145:465–470
- Dubinini MM (1960) The potential theory of adsorption of gases and vapors for adsorbents with energetically non-uniform surface. *Chem Review* 60:235–266
- Dubinini MM, Zaverina ED, Radushkevich LV (1947) Sorption and structure of active carbons I. Adsorption of organic vapors. *Zhurnal Fizicheskoi Khimii* 21:1351–1362
- Dupont L, Guillon E (2003) Removal of hexavalent chromium with a lignocellulosic substrate extracted from wheat bran. *Environ Sci Technol* 37(18):4235–4241
- Freundlich HMF (1906) Über die adsorption in losungen. *Z Phys Chem* 57(A):385–470
- Gordon C (1994) The use of cross-validation in neural network extrapolation of forest tree growth. *Proceedings of the Pattern Recognition Association of South Africa*, pp 1–12
- Gupta VK, Pathania D, Agarwal S, Sharma S (2013) Removal of Cr(VI) onto *Ficus carica* biosorbent from water. *Environ Sci Poll Res* 20: 2632–2644
- Gupta A, Majumder CB (2014) Adsorptive removal of chromium (VI) from aqueous solutions by using sugar and distillery waste material. *Int J Sci Engg Technol* 3:507–513
- Giwa AA, Bello IA, Oladipo MA, Adeoye DO (2013) Removal of cadmium from waste-water by adsorption using the husk of melon (*Citrullus lanatus*) seed. *Int J Basic Applied Sci* 2(1):110–123
- Gunay A, Arslankaya E, Tosun I (2007) Lead removal from aqueous solution by natural and pretreated clinoptilolite: adsorption equilibrium and kinetics. *J Hazard Mater* 146:362–371
- Hasan SH, Singh KK, Prakash O, Talat M, Ho YS (2008) Removal of Cr(VI) from aqueous solutions using agricultural waste ‘maize bran’. *J Hazard Mater* 152(1):356–365
- Ho YS, McKay G (2000) The kinetics of sorption of divalent metal ions onto sphagnum moss peat. *Water Res* 34(3):735–742
- Ho YS, McKay G, Wase DAJ, Foster CF (2000) Study of the sorption of divalent metal on peat. *Adsorp Sci Technol* 20(8):797–815
- Ho YS, McKay G (2002) Application of kinetic models to the sorption of copper(II) on to peat. *Adsorption Sci & Technol* 20(8):797–815
- Indian Standard (1991) Drinking water-specification (first revision), IS 10500
- Kondapalli S, Mohanty K (2009) Biosorption of hexavalent chromium from aqueous solutions by catla scales: equilibrium and kinetics studies. *Chem Eng J* 155(3):666–673
- Kondapalli S, Mohanty K (2011) Influence of temperature on equilibrium, kinetic and thermodynamic parameters of biosorption of Cr(VI) onto fish scales as suitable biosorbent. *J Water Resour Prot* 3(6): 429–439
- Krishna D, Sree R (2013) Response surface modeling and optimization of chromium (VI) removal from waste water using custard apple peel powder. *Walailak J Sci Technol* 11:489–496
- Kundu S, Gupta AK (2006) Arsenic adsorption onto iron oxide-coated cement (IOCC): regression analysis of equilibrium data with several isotherm models and their optimization. *Chem Eng J* 122:93–106
- Lagergren S (1898) Zur theorie der sogenannten adsorption gelöster stoffe. *Kungliga Svenska Vetenskapsakademiens, Handlingar* 24(4):1–39
- Langmuir I (1918) The adsorption of gases on plane surfaces of glass, mica and platinum. *J Am Chem Soc* 40(9):1361–1368
- Lopez-Núñez PV, Aranda-García E, Cristiani-Urbina MC, Morales-Barrera L, Cristiani-Urbina E (2014) Removal of hexavalent and total chromium from aqueous solutions by plum (*P. domestica* L.) tree bark. *Environ Eng Manag J* 13(8):1927–1938
- Malkoc E, Nuhoglu Y, Dundar M (2006) Adsorption of chromium(VI) on pomace—an olive oil industry waste: batch and column studies. *J Hazard Mater* 138(1):142–151
- Mauri R, Shinnar R, D Amore M, Giordano P, Volpe A (2001) Solvent extraction of chromium and cadmium from contaminated soils. *AICHE J* 47(2):509–512
- Mitra T, Singha B, Bar N, Das SK (2014) Removal of Pb(II) ions from aqueous solution using water hyacinth root by fixed-bed column and ANN modeling. *J Hazard Mater* 273:94–103
- Murphy V, Hughes H, McLoughlin P (2008) Comparative study of chromium biosorption by red, green and brown seaweed biomass. *Chemosphere* 70(6):1128–1134
- Nag S, Mondal A, Mishra U, Bar N, Das SK (2016) Removal of chromium(VI) from aqueous solutions using rubber leaf powder: batch, column studies and ANN modeling. *Desalin Water Treat* 57(36):16927–16942
- Namasivayam C, Yamuna RT (1995) Adsorption of chromium (VI) by a low-cost adsorbent: biogas residual slurry. *Chemosphere* 30(3):561–578
- Netzahuatl-Munoz AR, Aranda-García E, Cristiani-Urbina MC, Barragán-Huerta BE, Villegas-Garrido TL, Cristiani-Urbina E

- (2010) Removal of hexavalent and total chromium from aqueous solutions by *Schinus molle* bark. *Fresenius Environ Bull* 19(12): 2911–2918
- Netzahuati-Munoz AR, Guillién-Jiménez FM, Chávez-Gómez B, Villegas-Garrido TL, Cristiani-Urbina E (2012a) Kinetic study of the effect of pH on hexavalent and trivalent chromium removal from aqueous solution by *Cupressus lusitanica* bark. *Water Air Soil Pollut* 223(2):625–641
- Netzahuati-Munoz AR, Morales-Barrea LM, Cristiani-Urbina MC, Cristiani-Urbina E (2012b) Hexavalent chromium reduction and chromium biosorption by *Prunus serotina* bark. *Fresenius Environ Bull* 21(7):1793–1801
- Netzahuatitiani-Munoz AR, Cristiani-Urbina MC, Cristiani-Urbina E (2015) Chromium biosorption from Cr(VI) aqueous solutions by *Cupressus lusitanica* bark: kinetics, equilibrium and thermodynamic studies. *PLoS One* 10(9):e0137086. doi:10.1371/journal.pone.0137086
- Qaiser S, Saleemi AR, Umar M (2009) Biosorption of lead(II) and chromium(VI) on groundnut hull: equilibrium, kinetics and thermodynamics study. *Electronic J Biotech* 12:3–4
- Orhan Y, Büyüğüngör H (1993) The removal of heavy metals by using agricultural wastes. *Water Sci Technol* 28:247–257
- Özer A, Altundoğan HS, Erdem M, Tümen F (1997) A study on the Cr(VI) removal from aqueous solutions by steel wool. *Environ Pollut* 97(1–2):107–112
- Padilla AP, Tavani EL (1999) Treatment of industrial effluent by reverse osmosis. *Desalination* 126(1–3):219–226
- Patterson JW (1985) *Industrial wastewater treatment technology*, 2nd edn. Butterworth Publishers, Stoneham, MA, USA
- Pehlivan E, Altun TR (2008) Biosorption of chromium (VI) ion from aqueous solutions using walnut, hazelnut and almond shell. *J Hazard Mater* 155:378–384
- Polanyi M (1932) Section III—theories of the adsorption of gases. A general survey and some additional remarks. *Trans Faraday Soc* 28:316–333
- Rengaraj S, Joo CK, Kim Y, Yi J (2003) Kinetics of removal of chromium from water and electronic process wastewater by ion exchange resins: 1200H, 1500H and IRN97H. *J Hazard Mater* 102(2–3): 257–275
- Sarode DB, Jadhav RN, Khatik VA, Ingle ST, Attarde SB (2010) Extraction and leaching of heavy metals from thermal power plant fly ash and its admixtures. *Pol J Environ Stud* 19(6):1325–1330
- Şen A, Pereira H, Olivella MA, Villaescusa I (2015) Heavy metals removal in aqueous environments using bark as a biosorbent. *Int J Environ Sci Technol* 12(1):391–404
- Sharma DC, Forster CF (1994) A preliminary examination into the adsorption of hexavalent chromium using low-cost adsorbents. *Bioresor Technol* 47:257–264
- Singha B, Das SK (2011) Biosorption of Cr(VI) ions from aqueous solutions: kinetics, equilibrium, thermodynamics and desorption studies. *Colloids Surf B: Biointerfaces* 84(1):221–232
- Singha B, Naiya TK, Bhattacharya AK, Das SK (2011) Cr(VI) ions removal from aqueous solutions using natural adsorbents—FTIR studies. *J Environ Prot* 2(6):729–735
- Singha B, Das SK (2013) Adsorptive removal of Cu(II) from aqueous solution and industrial effluent using natural/agricultural wastes. *Colloids Surf B: Biointerfaces* 107:97–106
- Singh B, Bar N, Das SK (2014) The use of artificial neural networks (ANN) for modeling of adsorption of Cr(VI) ions. *Desalin Water Treat* 52(2014):415–425
- Singha B, Bar N, Das SK (2015) The use of artificial neural networks (ANN) for modeling of Pb(II) adsorption in batch process. *J Mol Liquids* 211:228–332
- Singh B, Bar N, Das SK (2014) The use of artificial neural networks (ANN) for modeling of adsorption of Cr(VI) ions. *Desalin Water Treat* 52(2014):415–425
- Temkin MI, Pyzhev V (1940) Kinetics of ammonia synthesis on promoted iron catalyst. *Acta Physicochim USSR* 12:327–356
- Tsoukalas LH, Uhrig RE (1997) *Fuzzy and neural approaches in engineering*. Wiley Interscience, New York, USA
- US Department of Health and Human Services (1991) *Toxicological profile for chromium*. Public Health Services Agency for the Toxic Substances and Diseases Registry, Washington
- Venkateswarlu P, Ratnam MV, Rao DS, Rao MV (2007) Removal of chromium from an aqueous solution using *Azadirachta indica* (neem) leaf powder as an adsorbent. *Int J Physical Sci* 2:188–195
- Wang XS, Chen LF, Li FY, Chen KL, Wan WY, Tang YJ (2010) Removal of Cr(VI) with wheat-residue derived black carbon: reaction mechanism and adsorption performance. *J Hazard Mater* 175:816–822
- Weber WJ, Morris JC (1963) Kinetics of adsorption on carbon from solution. *J San Eng Div* 89(2):31–60
- Wu YJ, Zhang LJ, Gao CL, Ma JY, Ma XH, Han RP (2009) Adsorption of copper ions and methylene blue in a single and binary system on wheat straw. *J Chem Eng Data* 54(12):3229–3234
- Yang Y (2007) Consistency of cross validation for comparing regression procedures. *Ann Stat* 35(6):2450–2473
- Zou W, Zhao L (2012) Removal of uranium(VI) from aqueous solution using citric acid modified pine saw dust: batch and column studies. *J Radioanal Nucl Chem* 292(2):585–595

Web sites

- <http://www.tfdpc.com/about2htm>. Accessed 5 May 2015
- <http://www.agri.tripura.gov.in/tripurahtm>. Accessed 1 May 2015